International Journal of Heat and Mass Transfer 176 (2021) 121469

Contents lists available at ScienceDirect

International Journal of Heat and Mass Transfer

journal homepage: www.elsevier.com/locate/hmt

Estimation of the through-plane thermal conductivity of polymeric ion-exchange membranes using finite element technique

V.M. Barragán[a], M.A. Izquierdo-Gil[a], J.C. Maroto[b], P. Antoranz[a], S. Muñoz[a,*]

[a] Department of Structure of Matter, Thermal Physics and Electronics, Complutense University of Madrid, Spain
[b] Department of Science, Computing & Technology, Universidad Europea de Madrid, Spain. Department of Electronics, Automation and Communications, Comillas Pontifical University, Madrid, Spain

ARTICLE INFO

Article history:
Received 28 February 2021
Revised 26 April 2021
Accepted 6 May 2021
Available online 1 June 2021

Keywords:
Ion-exchange membranes
Thermal conductivity
Finite element method

ABSTRACT

The aim of this study is to calculate the through-plane thermal conductivity of commercial polymeric ion-exchange membranes. Different membranes were considered to study the influence of membrane properties on the thermal conductivity values. In particular we focused on reinforcement, ion exchange capacity and membrane density and thickness. For this purpose, we use a simple experimental setup and a numerical simulation to estimate the thermal conductivity from the experimental temperature profiles. Once the system is calibrated, the model includes as the only unknown parameter the membrane thermal conductivity. To validate the method, the thermal conductivity of the well-known Nafion membranes has been determined, a very good agreement was achieved in context from reliable literature values. The study also provides the thermal conductivity of other polymeric ion-exchange membranes with great potential in diverse applications under non-isothermal conditions. The calculated thermal conductivity for the different ion-exchange membranes is in the range from 0.04 $Wm^{-1}K^{-1}$ to 0.42 $Wm^{-1}K^{-1}$. The results show that the reinforcement leads to lower values of thermal conductivity whereas a higher density or heterogenous structure leads to higher thermal conductivity values. The approach presented here, combining experimental and simulation techniques, may provide a basis for confirming the effect of the polymeric ion-exchange membrane properties on the thermal conductivity and may shed light on the best choice for the electrolyte of membrane-based applications performance under non-isothermal conditions.

1. Introduction

The development of renewable nontoxic and environment-friendly energies has promoted new energetic technologies such as those based on transport processes through polymeric ion-exchange membranes. Their applications spread through energy conversions devices such as fuel cells, reverse electrodialysis or polymer electrolyte membrane electrolyzer. All these applications share one common characteristic: a polymeric ion-exchange membrane used as electrolyte. Nowadays, these devices are still under development for an optimum performance to ensure stability and durability even under temperature changes. So, temperature has been confirmed as a relevant factor to ensure high performance of the device because any variation has an effect on each component of the fuel cell and essentially on the ion-exchange membrane as its properties depend on its degree of hydration. Therefore, a full knowledge of the temperature distribution inside the device may lead to more efficient designs and it has been the aim of a vast number of studies in the literature. Despite many different proton exchange membrane fuel cells (PEMFC) models have been extensively reported in the literature [1–5] to analyze the temperature distribution, very few of these dynamic studies include the temperature distribution. This could owe to the fact that scarce information about thermal properties, in particular the thermal conductivity, is available for polymeric ion-exchange membranes except for the Nafion membranes.

Thus, a better knowledge of the membrane properties, and in particular the thermal conductivity, is not only essential in heat transfer processes but it may be crucial for the selection of the membrane as electrolyte for predicting and understanding the energetic efficiency in applications under non-isothermal conditions.

* Corresponding author.
E-mail address: smsm@ucm.es (S. Muñoz).

https://doi.org/10.1016/j.ijheatmasstransfer.2021.121469

The classical Lee's disc method, has extensively probed as a simple tool to determine the thermal conductivity of materials with low thermal conductivity and polymers [6,7]. Some studies proposed modified and optimized Lee's disc apparatus [8] to overcome the limitations of the classical model. Other studies proposed alternative methods such as desalination techniques [9,10], the steady-state heat flow technique [11], or different direct measurements such as transient plane source method [12] or temperature profiles [13–16]. Precisely, when the temperature is known at least at two positions inside a heat-conducting solid, the Inverse Heat Conduction Technique (IHCP) [17–19] has revealed as an effective tool to estimate the thermal properties and the heat flux. New approaches optimized this technique to estimate temperature dependent properties [20,21]. Recently it is becoming increasingly widespread thanks to the successful results obtained in applications so different such as aerothermodynamics, renewal energies or even membranes including soft tissues [22–24]. All these methods shed light on new studies to estimate both thermal conductivity and contact resistance in different non-isothermal applications. In particular, the study of thermal conductivity and the contact resistance of fuel cells is a line of priority research and of great interest worldwide with new techniques emerging every day [25–29].

In this paper we propose a simple experimental setup in combination with a numerical simulation to estimate the thermal conductivity of commercial ion-exchange membranes.

Although numerical simulations have been proven as an adequate support for the previous performance of the membrane-based applications, to the best of our knowledge, no study has performed a finite element simulation to determine the thermal conductivity of ion-exchange membranes from the temperature profiles. We performed a stationary study using a parametric sweep to determine the thermal conductivity by fitting the simulated temperature profile to the experimental one.

2. Materials and methods

2.1. Experimental

2.1.1. Membranes

Different polymeric ion-exchange membranes have been analyzed in this work. Two homogeneous non-reinforced membranes, Nafion 115, Nafion 117, three heterogeneous membranes, Ralex AM(H) PES, Ralex CM(H) PES and MK 40, and three homogeneous membranes with reinforcement in their structure, Fumasep FKS-PET-75 and Selemion CSO with internal reinforcement, and Nafion N324, with external reinforcement.

Nafion 115 and Nafion 117 are homogeneous membranes consisting of a polytetrafluorethylene backbone and long fluorovinyl ether pendant side chains regularly spaced, terminated by a sulfonic acid group. Both have equivalent weight 1100 and a similar structure, but both differ in their thickness and specific weight. Ralex membranes possess basic binder on base of PE polyethylene with a fitting fabrics PES polyester and have also a similar structure, but AM(H) PES is an anion-exchange membrane while CM(H) PES is a cation-exchange membrane. MK-40 is a sulphonic polystyrene divinylbenzene membrane of heterogeneous type prepared by the inclusion of a finely ground ion-exchange resin in a polyethylene binder. In Fumasep FKS-PET-75, the polymer backbone is based on a hydrocarbon polymer material, with and internal PET reinforcement and in Selemion CSO the base polymer is St/DVB, with internal PVC reinforcement. Nafion N324 is a 0.15 mm thick Nafion membrane (with one layer having equivalent weight 1500 and thickness 0.0254 mm, and the other layer having equivalent weight 1100 and thickness 0.127 mm) fabric-reinforced with polytetrafluoroethylene fiber. The result is a "bimembrane" with a nominal thickness of 0.28 mm. Table 1 shows some properties of the studied membranes.

Membrane thickness was measured with a PCE-THM-20 material thickness meter with a resolution of 0.0002 mm. Final value of membrane thickness was obtained by averaging the results of at least ten measurements made at different points of the sample under study. The value of the membrane density was determined by measuring the area and the mass of each membrane samples. Results are also shown in Table 1.

Fig. 1 shows SEM (scanning electron microscope) images of the membranes used in this work. The images show important morphological differences between the different studied membranes.

2.1.2. Experimental device

Fig. 2 shows the device used to obtain the experimental temperature-time profiles. The device consisted of two copper cylinders, with the membrane sample positioned at the center and sandwiched between both cylinders in a symmetrical manner. In their external face, the cylinders had an orifice to permit the inlet and outlet streams of water at a controlled selected temperature. In these experiments, water was only made circulate in one of the cylinders. The external face of the other cylinder was in contact with air at ambient temperature. A holder permitted to accommodate the cylinders in horizontal position and kept the membrane sample sandwiched between them. The apparatus was designed to give a one-dimensional heat flux. For this purpose, they were thoroughly insulated in the radial direction with an insulated shell.

Three holes were made, spaced at intervals of 1 cm, in each copper cylinder. Pt100 sensors were placed inside each hole, to measure the temperature at this position. Thus, temperature was measured in six points, as it is shown in Fig. 2a. T_1 corresponds to the nearest value to the hot water inlet, and the rest were numbered sequentially. Thus, sensors T_3 and T_4 correspond to the temperatures measured next to the membrane on its two sides. The ambient temperature was measured by placing a digital thermometer around the device. Changes in ambient temperature were recorded and monitored in some of the experiments.

The procedure followed to determine the temperatures in the stationary state was the same for all the samples analyzed. The membrane sample was always positioned between the two cylinders. When the temperature of the water bath reached the selected value, the water started to circulate through one of the cells using the corresponding orifice, and the temperature was recorded during a time interval between 4 and 5 hours. This interval time was previously assessed as the one required to reach the steady state. A first measurement was made with the cell without the insulating cover and without any membrane located between the two cylinders (Fig. 2a), to verify and calibrate the model of the numerical simulation.

2.2. Finite element simulations

To determine the through-plane thermal conductivity of the tested membranes, we have used Comsol Multiphysics® (Comsol Inc., Burlington, MA, USA) that implements the FE numerical technique. Thus, we calculate the temperature profiles at the same six positions measured with the experimental setup. A simple model with no isolation, was designed to validate the experimental setup, denoted as SysCu, from now on. The model consists of two identical solid copper cylinders with a radius of 2.5 cm and a height of 3 cm. The system is placed horizontally with both cylinders stuck without gap between them. Six holes with a diameter of 0.5 cm, are designed to simulate the Pt100 Sensors. Temperature probes are placed inside these holes to determine the temperature values, denoted as T_i, i=1 to 6. Unlike experimental sensors, these probes

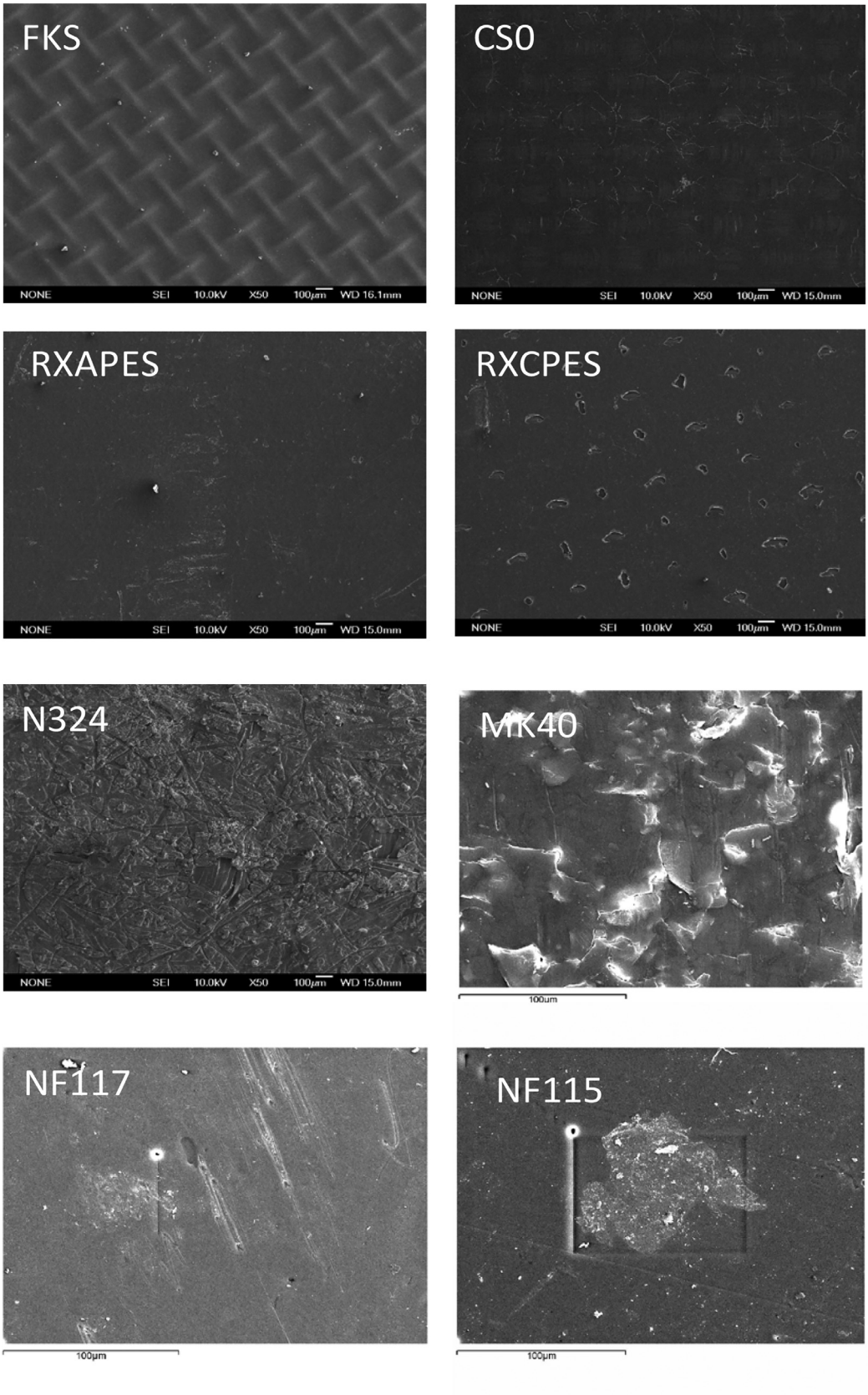

Fig. 1. SEM images of the membranes used in this work (Spanish National Centre for Electron Microscopy ICTS).

Table 1
Properties of the ion-exchange membranes used in this work. (*Provided by the manufacturer. ** Measured.).

Membrane	Short Name	Structure	IEC*(eq kg^{-1})	$\rho^{**}(10^3 kg\ m^{-3})$	$d^{**}(10^{-6}\ m)$
Nafion 115	NF115	Homogeneous Non-reinforcement	0.96	2.00	131
Nafion 117	NF117	Homogenous Non-reinforcement	0.94	1.98	186
Selemion CSO	CSO	Homogeneous Internal reinforcement	2.0	1.30	80.6
Fumasep FKS-PET-75	FKS	Homogeneous Internal reinforcement	0.9	1.00	94.1
Nafion N324	N324	Homogeneous External reinforcement	1.1	1.55	271
MK-40	MK40	Heterogeneous	2.6	1.12	450
Ralex CM(H) PES	RXCPES	Heterogeneous	2.34	0.82	431
Ralex AM(H) PES	RXAPES	Heterogeneous	1.97	0.94	454

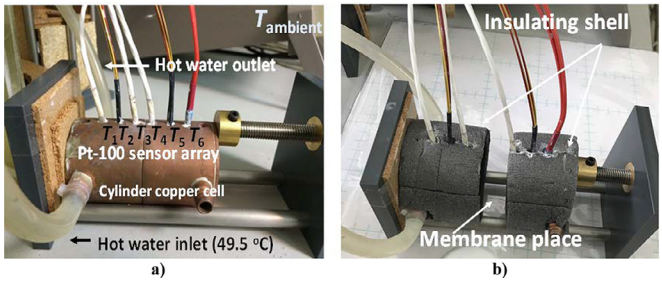

a) b)

Fig. 2. Experimental cell used to measure stationary temperatures. a) Configuration used to calibrate the device (without external insulating shell and without membrane). b) The device with the external insulating shell.

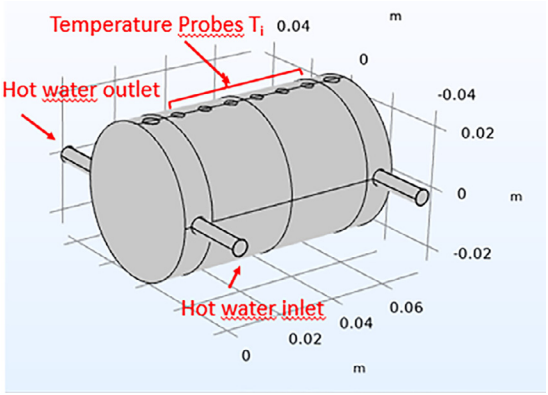

Fig. 3. Model designed in Comsol.

may provide, the minimum, the maximum and the average temperature value along the hole. In addition, the numerical simulation may include probes to measure temperature at both sides of the membrane under test so the experimental setup was not able to provide these values. The outer temperature is fixed at the experimental ambient temperature. Two additional hollow cylinders located perpendicular to left and to right of the system with same radius, 0.2 cm, represent the hot water inlet and outlet and the cylinder at ambient temperature. In most cases the ambient temperature was about 293.15K but the simulation allows to consider a possible temperature interval that accounts for sudden changes observed during some measurements. A stationary study with a parametric swept was performed using the Heat Transfer Module of Comsol. The iterative process of fitting the calculated temperature profile to the experimental one, determines the thermal properties of the solid materials used in the experimental model. Fig. 3 shows the model designed in Comsol.

Table 2
Properties of the materials used for the calibration model in the numerical simulation.

Properties	Cu	Insulating Shell
Density ($kg.m^{-3}$)	8962	298
Thermal Conductivity ($W.m^{-1}.K^{-1}$)	388	0.035
Heat Capacity at constant pressure ($J.kg^{-1}.K^{-1}$)	385	1880

Then, we proceed to add the insulating shell of polyethylene around the system. This insulating shell consists of two hollow cylinders with same radius, 2.5 cm, and thickness of 1 cm. This system is denoted as SysInsCu, from here on out. A similar procedure leads to check the thermal properties of the insulating material provided by the manufacturer. Table 2 shows the properties used for the material of the experimental setup.

Once the system has been characterized, the membrane is placed between both cylinders with no gap between them and without any membrane holder. The membrane samples were simulated as a cylinder of the same radius of the cylinders and the thickness of the membrane as height. All membranes were dry. The membrane is set as a thin thermally resistive layer in the numerical modeling. Both sides of membrane were modeled as thermal contacts. Each contact was considered as a thin resistive layer with a thermal conductivity and a thickness. In our study the thickness was known but the thermal conductivity was the unknown parameter. A finite element mesh was built for our model. In order to generate a precise description of the temperature gradient along the model, each tetrahedron must occupy a region that is small enough for the gradient to be adequately interpolated from the nodal values. Therefore, there is a compromise between the size of the finite element mesh, the level of accuracy and computing resources. Due to the fact that the dimension involved in the different parts of the system vary by several orders of magnitude (microns for the membrane compared with millimeters for both external cylinders), an adaptative mesh is used so that the size of the basic tetrahedron is varied for the different regions. Therefore, in order to obtain an accurate result for the temperature gradient within the membrane, the number of tetrahedra in this region had to be considerably higher (~80000 for the membrane) than the corresponding number for the region occupied by both copper cylinders (~12000). We performed again a similar iterative process considering the membrane thermal conductivity as the only unknown variable for the simulation. Each one of the systems with the membrane are denoted as the corresponding membrane name, for example: NF117, NF115, etc. In our numerical modeling, we can also consider the possible convection losses due to the flow of water to the left of the device. The main sources of convection losses in our model were the hot water circulating through the cylinder

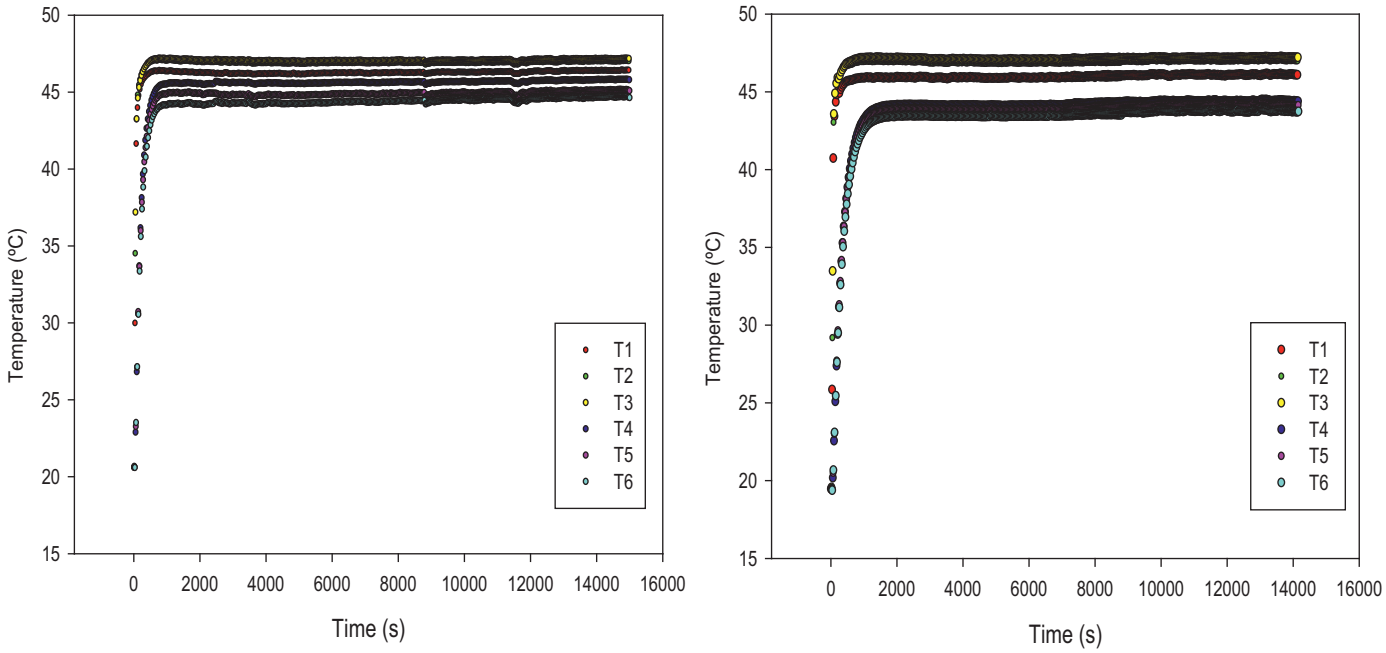

Fig. 4. Temperature-time curves obtained for (a) copper cell without the insulating layer and without the membrane (b) MK-40 membrane.

to the left of the model and the external cylinder. The former is modelled as a forced convection consisting of a long horizontal tube with water circulating at a velocity of 0.51m/s at the bath temperature. The outer cylinder was modelled as external natural convection of a long horizontal cylinder and the rest of the boundaries were opened at ambient temperature. In view of the results shown later on, the effect of these losses may be of great importance to understand the experimental results.

To validate this method as a tool to estimate the thermal conductivity of polymeric ion-exchange membranes, we have chosen the Nafion membranes, NF117 and NF115, as tests standard because their thermal properties are well documented in the literature.

The advantages of the proposed method are twofold: firstly, it is not necessary a previous calculus neither the heat flux nor the thermal contact resistances; secondly the required membrane surface is small and only the knowledge of the membrane density and thickness is enough to estimate the thermal conductivity. Although this study has focused on thin membranes, we would like to point out that the approach presented here may be applicable to determining the thermal properties of any other membrane or even of any other solid material.

3. Results and discussion

3.1. Experimental temperature-time profiles

Fig. 4 shows, as examples, the experimental temperature-time values for two of the studied cases. The curves shown in Fig. 4a depict the results obtained with the copper cell, without the insulating layer and without the membrane, whereas the curves of Fig. 4b depict the temperature-time profiles obtained with the heterogeneous membrane MK40. Similar results were obtained with all the tested membranes. As it can be observed, temperature-values show an initial transitory trend with time followed by a stationary-state. A gap was observed between T_3 and T_4 depending on the tested membrane.

The stationary temperature in each point was obtained by averaging the results measured with the corresponding sensor from a time of 8000 s. The standard deviation was always less than 0.2 in the most unfavorable case, with values of the order of 10^{-2} in the most of cases studied. Table 3 shows the stationary temperature obtained as a function of the position in the cell for each case studied.

Table 3
Stationary temperature values measured with the six Pt100 Sensors for some of the different systems studied: the SysCu, SysInsCu and for the Nafion membranes NF117 and NF115.

SystemPt100 Sensors	SysCu	SysInsCu	NF117	NF115
T_1 (K)	322.50	319.48	320.13	320.23
T_2 (K)	322.24	320.13	320.47	320.78
T_3 (K)	322.42	320.30	320.42	321.15
T_4 (K)	321.03	318.88	318.30	319.48
T_5(K)	320.85	318.14	317.83	319.66
T_6 (K)	320.62	318.14	317.51	317.87

3.2. Simulated temperature profiles and thermal conductivity

We calculated the temperature profile and the temperature gradient for the model with membrane designed in Comsol, for each parametric sweep under stationary state. The temperature distribution in the device is shown in Fig. 5a. The presence of the membrane leads to a significant temperature gradient as it is shown in Fig. 5b, as example, for the Nafion membranes NF117 and NF115.

Fig. 6 shows the different temperature profiles obtained for the calibration systems: SysCu (a) and SysInsCu(b) and for the Nafion membranes, NF117(c) and NF115(d). The results for the different membranes studied are shown in Fig. 7.

The relative difference between simulated and experimental temperatures was between 0 and 0.25 % in the most unfavorable case. We have estimated the contact resistances to assure that the measured temperature differences at both sides of the membrane samples are primarily due to the membrane thermal resistance. From these data, we have estimated the temperatures difference due to the contact resistances for Cu-Cu and Cu-Nafion membranes. We found a temperatures difference of 0.11 K for Cu-Cu and 0.07 K and 0.12 K for Nafion 115 and Nafion 117, respectively.

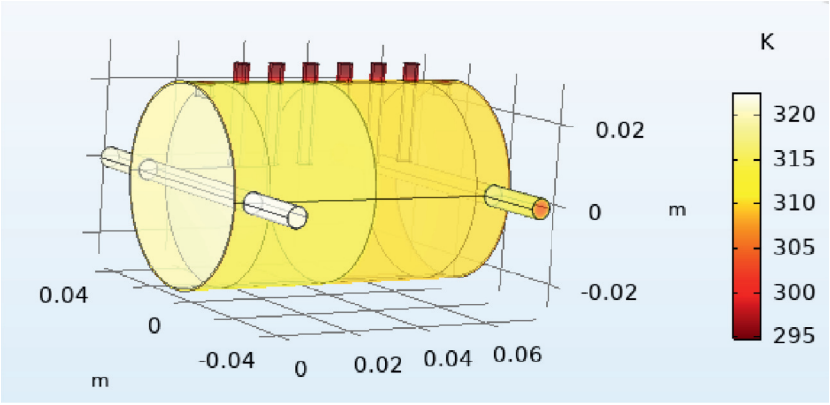

a)

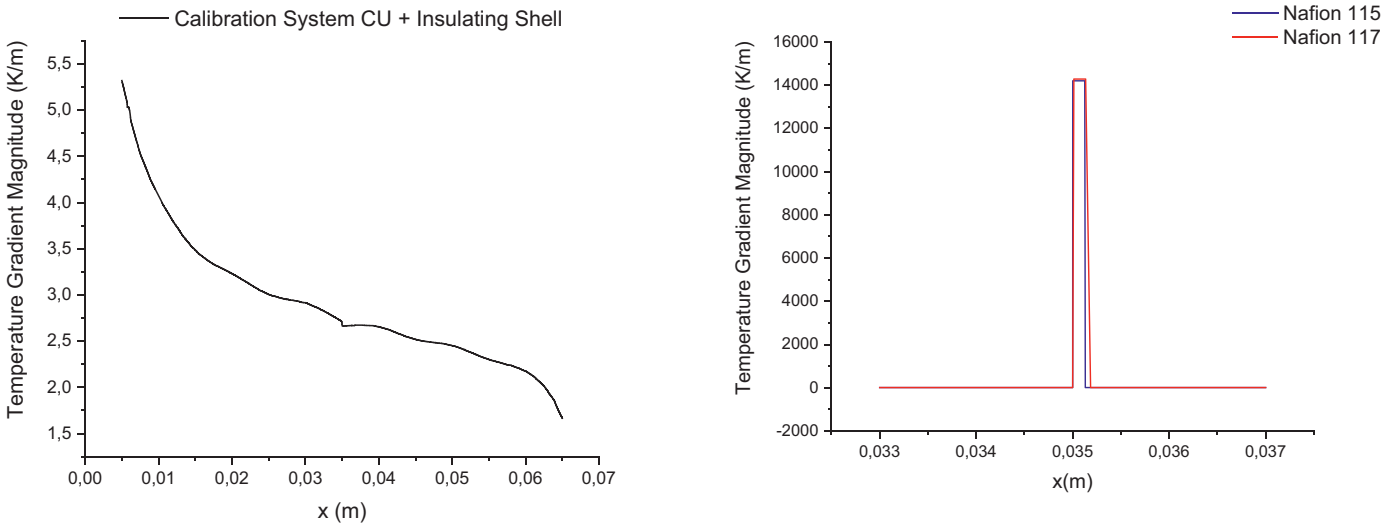

b)

Fig. 5. a) Temperature distribution obtained for copper cell with the insolating layer and the membrane (b) Temperature gradient magnitude obtained for copper cell (left graph) and for the system with membranes Nafion 117 and 115 (right graph).

A comparison between these values and the experimental temperature differences points out that the relative contribution of the contacts represents less than 8% of the temperatures difference for Cu-Cu and about a 5% for Nafion membranes. These results may confirm that the temperature differences measured next to both sides of the thermal contact are primarily due to the thermal resistance and not to other factors such as interfacial contact resistance. As it is shown, some points of the experiments are not well fitted to the corresponding simulated value. We think that this may be an artifact due to accidental shifts of the sensor during the measurement.

The presence of the insulating shell led to an increasing trend to the left of the experimental system whereas a decreasing trend, similar to the obtained for the calibration system, is always obtained to the right of the membrane. This change of trend may be due to the convection losses on the tube used to circulate the hot water. The temperature difference between the solid copper cylinders increases for the different membranes with respect to the system without membrane, thus, the more difference the less thermal conductivity.

Table 4
Thermal conductivity of the membranes studied.

Membrane	Thermal Conductivity (W/m.K)
Nafion 115	0.22
Nafion 117	0.25
Selemion CSO	0.04
Fumasep FKS-PET-75	0.38
Nafion N324	0.11
MK 40	0.42
Ralex CM(H) PES	0.26
Ralex AM(H) PES	0.24

A later optimization fits the simulated temperature profile to the experimental temperature values at the six positions of the Pt100 Sensors. This fitting provides the thermal conductivity estimated for each membrane. In our model we set the thermal conductivity value with a maximum of two significant digits. Table 4 shows the thermal conductivity values obtained for each membrane from these fittings.

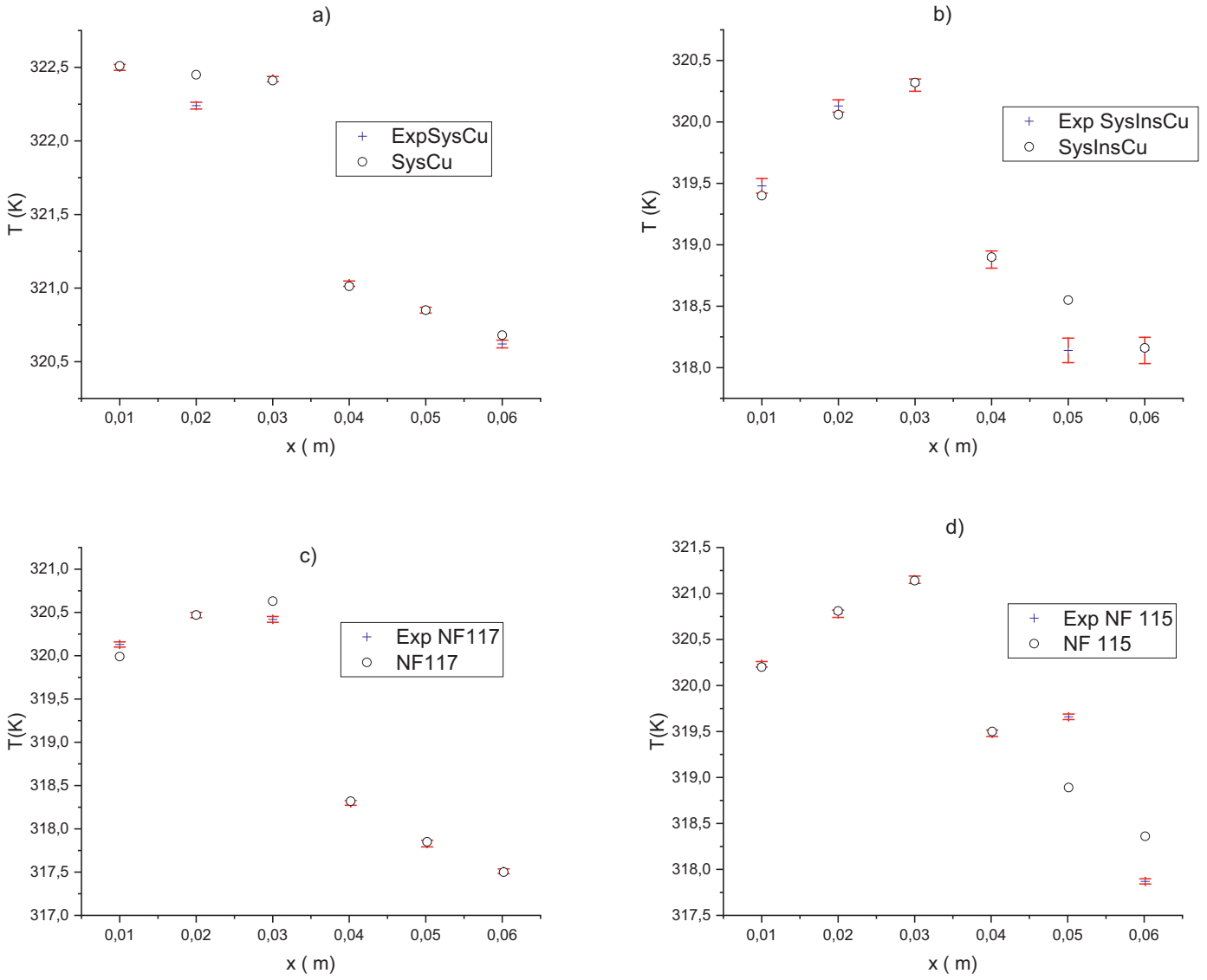

Fig. 6. Experimental and simulated temperature profiles obtained for the calibration systems: SysCu and SysInsCu, and for the Nafion membranes NF117 and NF115.

The thermal conductivity values estimated for the different membranes studied, are in the range from 0.04 $Wm^{-1}K^{-1}$ to 0.42 $Wm^{-1}K^{-1}$. The highest value is obtained for the MK40, a heterogeneous membrane with a polyethylene binder. The value obtained is in the range from 0.33 to 0.5 $Wm^{-1}K^{-1}$ [30], provided for the polyethylene conductivity, and it may explain the high value obtained. The value obtained for Fumasep membrane agrees with typical values for thermal conductivity of hydrocarbon polymers, in the range from 0.12-0.52 $Wm^{-1}K^{-1}$ [30]. However, the lowest value is obtained for the Selemion membrane, a monovalent selective cation exchange membrane that contains a thin polyethyleneimine anion exchange layer. This low value is in the range from 0.03 to 0.04 $Wm^{-1}K^{-1}$ [30] reported as typical values for the thermal conductivity of polystyrene.

We have studied three Nafion membranes: NF115, NF117 and NF324. The values obtained for the NF117 and NF115 membranes, 0.25 $Wm^{-1}K^{-1}$ and 0.22 $Wm^{-1}K^{-1}$ respectively, validate this method to estimate the thermal conductivity of thin membranes so the values obtained are in good agreement with those reported in the literature for these well-known membranes that varied in the interval 0.1-0.25 $Wm^{-1}K^{-1}$ depending on the used method [12,31–34]. The comparison between NF115 and NF117 seems to confirm that higher density and lower thickness lead to lower thermal conductivity values at least for the Nafion membranes. Unlike NF115 and NF117, NF 324 is a teflon fabric reinforced membrane. Thus, the results confirm a lower value for the NF324 conductivity due to the presence of this reinforcement.

In the medium range of the values obtained, are the thermal conductivity of the two Ralex membranes studied. We considered a cationic (RXCPES) and an anionic (RXAPES) to study the effect on the thermal conductivity. Both membranes are composites formed from ion-exchange resins with polyethylene basic binder with a reinforcement of a polyester fitting fabric. The results confirm that cationic membrane has lower value than the corresponding anionic one, probably due to its higher density.

Fig. 8 presents both ion-exchange capacity and through thermal conductivity for the studied membranes. No relation can be observed between these two membrane properties. We may conclude that membrane structure is the most important factor that explains differences in the thermal conductivity of dry membranes.

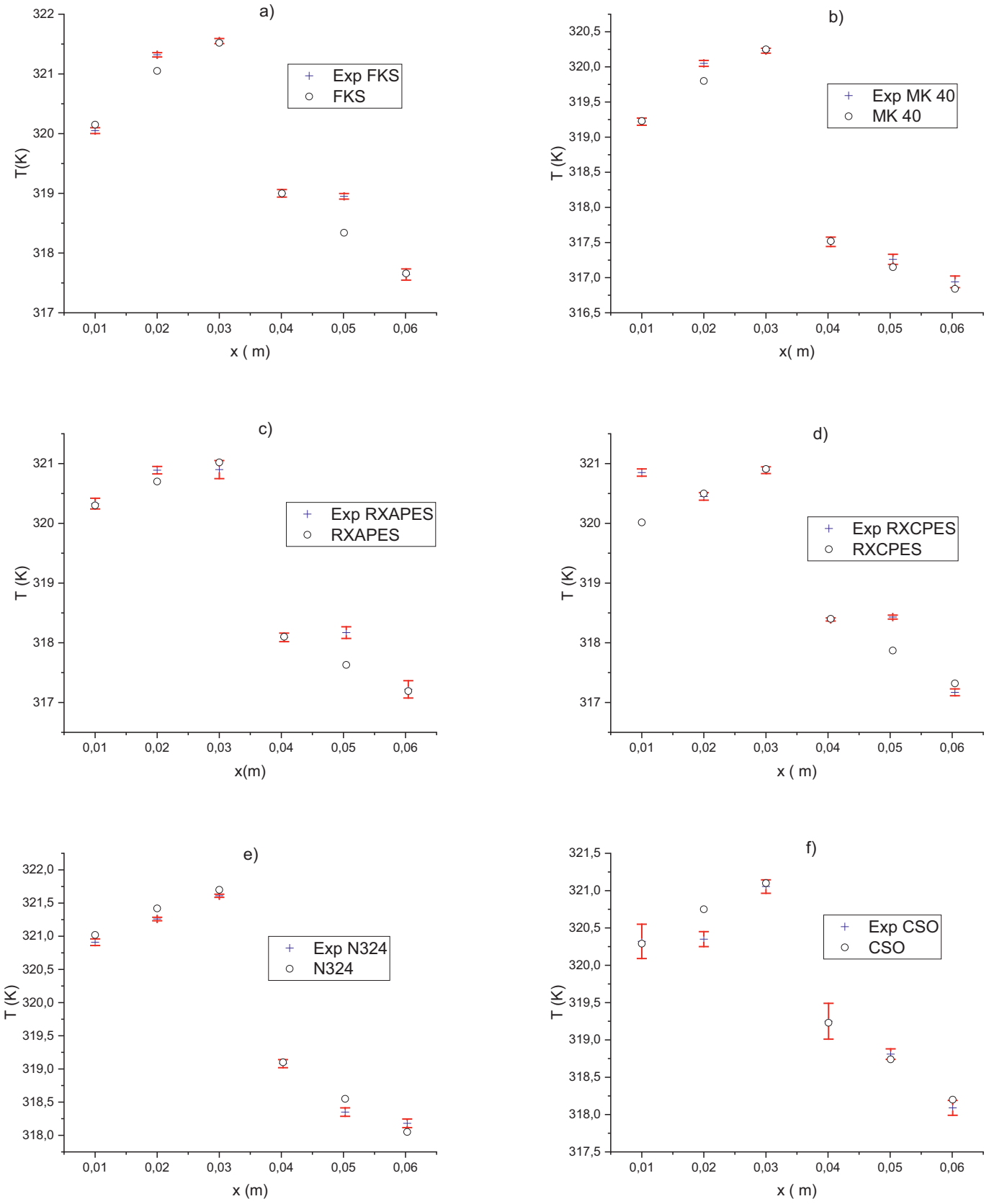

Fig. 7. Experimental and simulated temperature profiles obtained for the different membranes studied.

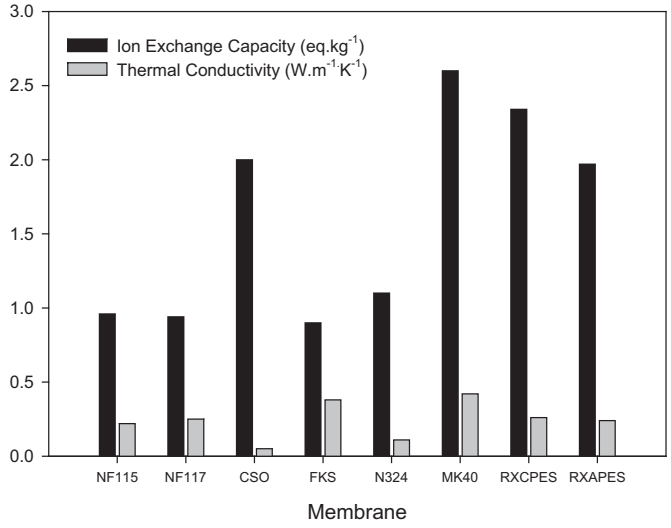

Fig. 8. Ion exchange capacity (given by the manufacturer) and through thermal conductivity (estimated in this study) for the different membranes studied.

4. Conclusions

Combination of analytical (finite elements) and experimental (temperature profiles) techniques shows to be a valid approach to the characterization of the thermal properties of commercial polymeric ion-exchange membranes. The above experimental results point out the capability of the proposed setup system to detect the thermal conductivity of ion-exchange membranes from temperature profiles and a simple experimental setup. Thus, the thermal conductivity is determined with the only requirement that the membrane density and thickness are known. The proposed method is validated with the excellent agreement achieved for the Nafion membranes in context from reliable literature values. The results obtained for the different ion-exchange membranes studied, confirmed the influence of the reinforcement and the membrane density and thickness on the thermal conductivity values. The reinforcement always led to lower thermal conductivity values. A comparison between the different membranes structure, according to homogeneous, reinforced or heterogenous, concluded that the lowest values correspond to the tested homogenous reinforced membrane. Thus, the membrane structure seemed to be the most relevant factor on the thermal conductivity value. The model designed may provide in addition to the thermal conductivity, other magnitudes of interest such as the heat flow or the contact resistance that may shed light on new studies to better and more efficient membrane-based devices.

Declaration of Competing Interest

The authors declare that they have no known competing financial interests or personal relationships that could have appeared to influence the work reported in this paper.

CRediT authorship contribution statement

V.M. Barragán: Conceptualization, Methodology, Validation, Formal analysis, Investigation, Resources, Writing - review & editing, Visualization, Funding acquisition. **M.A. Izquierdo-Gil:** Validation, Writing - review & editing. **J.C. Maroto:** Validation, Formal analysis, Writing - review & editing. **P. Antoranz:** Validation, Writing - review & editing. **S. Muñoz:** Methodology, Validation, Software, Writing - original draft, Writing - review & editing, Visualization, Funding acquisition.

Acknowledgments

Financial support of this work by Banco de Santander and Universidad Complutense de Madrid within the framework of Projects: PR75/18-21589, PR108/20-02 and the Project for Research Groups (Bioelectromagnetism Research Group 910305) are gratefully acknowledged.

References

[1] H. Ju, H. Meng, C.Y. Wang, A single-phase, non-isothermal model for PEM fuel cells, Int. J. Heat Mass Transf. 48 (7) (2005) 1303–1315.
[2] G. Zhang, J. Wu, Y. Wang, Y. Yin, K. Jiao, Investigation of current density spatial distribution in PEM fuel cells using a comprehensively validated multi-phase non-isothermal model, Int. J. Heat Mass Transf. 150 (2020) 119294.
[3] Y. Shan, S.Y. Choe, A high dynamic PEM fuel cell model with temperature profiles, J. Power Sour. 145 (1) (2005) 30–39.
[4] S. Um, C.Y. Wang, Computational study of water transport in proton exchange membrane fuel cells, J. Power Sour. 156 (2) (2006) 211–223.
[5] E. Sadeghi, N. Djilali, M. Bahrami, Effective thermal conductivity and thermal contact resistance of gas diffusion layers in proton exchange membrane fuel cells. Part 1: effect of compressive load, J. Power Sour. 196 (2011) 246–254.
[6] M.C. García-Payo, M.A. Izquierdo-Gil, Thermal resistance technique for measuring the thermal conductivity of thin microporous membranes, J. Phys. D: Appl. Phys. 37 (2004) 3008–3016.
[7] P. Philip, L. Fagbenle, Design of Leeś disc electrical method for determining thermal conductivity of a poor conductor in the form of a flat disc, Int. J. Innovation Sci. Res. (2014) 335–343 ISSN 2351-8014 Vol. 9 No. 2 Sep..
[8] N. Sombatsompop, A.K. Wood, Measurement of thermal conductivity of polymers using an improved Lee's Disc apparatus, Polym. Test. 16 (3) (1997) 203–223.
[9] F.Y.C. Huang, R. Reprogle, Thermal conductivity of polyvinylidene fluoride membranes for direct contact membrane distillation, Environ. Eng. Sci. 36 (4) (2019) 12–31.
[10] J. Vanneste, J.A. Bush, K.L. Hickenbottom, C.A. Marks, D. Jassby, C.S. Turchi, T.Y. Cath, Novel thermal efficiency-based model for determination of thermal conductivity of membrane distillation membranes, J. Membr. Sci. 548 (2018) 298–308.
[11] G. Unsworth, N. Zamel, X. Li, Through-plane thermal conductivity of the microporous layer in a polymer electrolyte membrane fuel cell, Int. J. Hydrogen Energ. 37 (2012) 5161–5169.
[12] M. Ahadi, M. Andisheh-Tadbir, M. Tam, M. Bahrami, An improved transient plane source method for measuring thermal conductivity of thin films: deconvoluting thermal contact resistance, Int. J. Heat Mass Transf. 96 (2016) 371–380.
[13] O.S. Burheim, H. Su, H.H. Hauge, S. Pasupathi, B.G. Pollet, Study of thermal conductivity of PEM fuel cell catalyst layers, Int. J. Hydrogen Energ. 39 (2014) 9397–9408.
[14] P.J.S. Vie, S. Kjelstrup, Thermal conductivities from temperature profiles in the polymer electrolyte fuel cell, Electrochim. Acta 49 (2004) 1069–1077.
[15] O. Burheim, H. Su, S. Pasupathi, J.G. Pharoah, B.G. Pollet, Thermal conductivity and temperature profiles of the micro porous layers used for the polymer electrolyte membrane fuel cell, Int. J. Hydrogen Energ. 38 (2013) 8437–8447.
[16] R. Bock, H. Karoliussen, F. Seland, B.G. Pollet, M.S. Thomassen, S. Holdcroft, O.S. Burheim, Measuring the thermal conductivity of membrane and porous transport layer in proton and anion exchange membrane water electrolyzers for temperature distribution modelling, Int. J. Hydrogen Energ. 45 (2) (2020) 1236–1254.
[17] Y.C. Hon, T. Wei, A fundamental solution method for inverse heat conduction problem, Eng. Anal. Bound. Elem. 28 (2004) 489–495.
[18] J.V. Beck, Nonlinear estimation applied to the nonlinear inverse heat conduction problem, Int. J. Heat Mass Transf. 13 (1970) 703–716.
[19] M. Monde, Analytical method in inverse heat transfer problem using Laplace transform technique, Int. J. Heat Mass Transf. 43 (2000) 3965–3975.
[20] B. Blackwell, J.V. Beck, A technique for uncertainty analysis for inverse heat conduction problems, Int. J. Heat Mass Transf. 53 (2010) 753–759.
[21] M. Cui, X. Gao, J. Zhang, A new approach for the estimation of temperature-dependent thermal properties by solving transient inverse heat conduction problems, Int. J. Therm. Sci. 58 (2012) 113–119.
[22] T. Liu, J. Montefort, S. Stanfield, S. Palluconi, J. Crafton, Z. Cai, Inverse heat transfer methods for global heat flux measurements in aerothermodynamics testing, Prog. Aerosp. Sci. 107 (2019) 1–8.
[23] A.S. Vaka, P. Talukdar, Novel inverse heat transfer technique for estimation of properties and location-specific process parameters of roof-mounted solar PV plants, Therm. Sci. Eng. Prog. 19 (2020) 100657.
[24] P. Seshaiyer, J.D. Humphrey, A sub-domain inverse finite element characterization of hyperelastic membranes including soft tissues, ASME J. Biomech. Eng. 125 (3) (2003) 363–371.
[25] N. Zamel, J. Becker, A. Wiegmann, Estimating the thermal conductivity and diffusion coefficient of the microporous layer of polymer electrolyte membrane fuel cells, J. Power Sour. 207 (2012) 70–80.
[26] A. Irace, P.M. Sarro, Measurement of thermal conductivity and diffusivity of single and multilayer membranes, Sens Actuators 76 (1999) 323–328.

[27] R. Bock, H. Karoliussen, F. Seland, B.G. Pollet, M.S. Thomassen, S. Holdcroft, O.S. Burheim, Measuring the thermal conductivity of membrane and porous transport layer in proton and anion exchange membrane water electrolyzers for temperature distribution modelling, Int. J. Hydrogen Energ. 45 (2020) 1236–1254.
[28] A.J. Chapman, Heat Transfer, The Macmillan Company, New York, 1960.
[29] C.I. Idumah, A. Hassan, Recently emerging trends in thermal conductivity of polymer nanocomposites, Rev. Chem. Eng. 32 (2016) 413–457.
[30] J.E. Mark, Physical Properties of Polymers Handbook, Springer, New York, 2007.
[31] M. Khandelwal, M.M. Mench, Direct measurement of through-plane thermal conductivity and contact resistance in fuel cell materials, J. Power Sour. 161 (2006) 1106–1115.
[32] N. Alhazmi, D.B. Ingham, M.S. Ismail, K. Hughes, L. Ma, M. Pourkashanian, The through-plane thermal conductivity and the contact resistance of the components of the membrane electrode assembly and gas diffusion layer in proton exchange membrane fuel cells, J. Power Sour. 270 (2014) 59–67.
[33] O. Burheim, P.J.S. Vie, J.G. Pharoah, S. Kjelstrup, Ex situ measurements of through-plane thermal conductivities in a polymer electrolyte fuel cell, J. Power Sour. 195 (2010) 249–256.
[34] C.L. Choy, Y.W. Wong, G.W. Yang, T. Kanamoto, Elastic modulus and thermal conductivity of ultra drawn polyethylene, J. Polym. Sci. Part B: Polym. Phys. 37 (1999) 3359–3367.